

Adjoint Power Flow Analysis for Evaluating Feasibility

Marko Jereminov¹, *Graduate Student Member, IEEE*, David M. Bromberg², *Member, IEEE*,
Amritanshu Pandey¹, *Graduate Student Member, IEEE*, Martin R. Wagner¹, *Graduate Student
Member, IEEE*, and Larry Pileggi¹, *Fellow, IEEE*

Abstract—Recently it has been demonstrated that the equivalent circuit formulation for modeling and simulation of the AC Power Flow (AC-PF) problem can be used to improve the convergence properties and to facilitate scaling to large system sizes (80k+ buses). The nonlinear nature of the power flow formulation, however, still maintains the problem of identifying infeasibility – system configurations with no solution. In this paper we introduce the Adjoint Power Flow formulation to evaluate the power flow feasibility. Infeasibility current source models are added to the system model to capture KCL (Kirchhoff’s Current Law) violations within the power flow circuit problem as non-zero voltages in the adjoint (dual) circuit. We show that the solution of the Adjoint Power Flow circuit corresponds to the optimal currents needed to achieve feasibility for an infeasible system case.

Index Terms— adjoint power flow, circuit formalism, equivalent split-circuit, feasibility analysis, optimization circuits

I. INTRODUCTION

Alternating Current Power Flow (AC-PF) is a nonlinear steady-state problem formulated to determine the power system operating point at a fixed frequency, and as such it represents a fundamental component in everyday operation and planning of electrical power systems. Despite the lack of convergence robustness [1], AC-PF remains the industry standard for transmission level power grid analyses. In contrast to the actual power system, where the grid frequency changes slightly with a demand change, and control systems adjust the generated power to maintain a frequency close to the nominal one [2], the corresponding power flow problem generally incorporates one or more slack bus generators to represent the additional power that is needed. The real and reactive powers supplied by a slack bus are unbounded, however, the formulated power flow problem can still be infeasible since it is conceivable, due to the nonlinearities and system topology, that the slack generators may not be able to provide additional power to all locations. This, along with formulations that have distributed slack buses (to model AGC or droop control), can result in divergence of the numerical algorithms used to obtain the power flow solution (Newton Raphson, Gauss-Seidel, etc.).

Recent advances in the simulation and modeling of power systems have included the equivalent split-circuit formulation [3]-[6]. It was demonstrated that circuit formalism can be

utilized to allow for adaptation and application of methods and algorithms from the circuit simulation field [7]-[8] to improve convergence properties and scale to large system sizes [5]. Importantly, any generalized model of existing and emerging grid technologies can be incorporated within the simulation framework without loss of generality [9]. However, the power flow simulation problem remains nonlinear due to models that define constant power components in this formulation [3]-[4]. Moreover, since divergence cannot be avoided when the power system problem is infeasible, it is difficult to distinguish systems that have diverged due to a “tool’s lack of robustness” from those that are “truly infeasible”

There have been attempts to tackle the detection of power flow infeasibility. In [10], the authors discussed the conditions that define the upper bound on the number of feasible power flow solutions based on the network topology, while [11] introduces a predictor-corrector technique to explore the feasible solution space of power flow. Various homotopy methods such as the Continuation Power Flow method (CPF) [12] are proposed to solve the continuous sequence of power flow problems while changing the loading factor of the system to detect the point of system collapse. Furthermore, the two sufficient conditions for which the power flow problem does not have a solution based on semidefinite relaxation of power flow and reactive power limits are presented in [13].

One approach that attempted to identify and correct the power flow infeasibility was presented in [14], where the author formulated the power flow problem in terms of a least squares minimization to quantify the insolubility. The approach is described as finding a solvable boundary and the best direction to shed the loads for restoring the feasibility, but was shown to suffer from divergence problems [15] and lead to errors introduced by the solution [16]. Therefore, the goal remains to create a generalized, scalable, and efficient framework that not only detects infeasibility, but accurately provides spatial information to identify locations and/or causes of network infeasibility.

As an alternative method for constructively solving the power flow problem, the noniterative “Holomorphic Embedding Load-Flow Method” (HELM) [17] is purported to find a correct power flow solution if one exists. However, the approach as presently described handles only PQ buses, and has

This work was supported in part by the Defense Advanced Research Projects Agency (DARPA) under award no. FA8750-17-1-0059 for the RADICS program, and the National Science Foundation (NSF) under contract no. ECCS-1800812.

¹Authors are with the Department of Electrical and Computer Engineering, Carnegie Mellon University, Pittsburgh, PA 15213 USA (e-mail: {mjeremin, amritanp, mwagner, pileggi}@andrew.cmu.edu).

²Author is with Pearl Street Technologies, (e-mail: bromberg@pearlstreettechnologies.com).

significant issues with accurately modeling PV buses [18]. Furthermore, the presented algorithms do not seem to scale well to large power flow systems [18].

In this paper we introduce the Adjoint Power Flow analysis as an extension of the equivalent split-circuit power flow formulation. It is shown that the KCL violation currents that arise for an infeasible system as a consequence of over-constraining the governing circuit equations can be captured by the adjoint (dual) power flow circuit of the original problem. Therefore, infeasibility can be optimally identified by solving both the original system and its adjoint system. A significant contribution is the extension of adjoint (dual) circuit theory to steady-state power system analysis at a fixed frequency. In addition to optimally capturing the infeasibility of a power flow problem, the coupled power flow and adjoint circuits represent a generic framework for any power system optimization problem. Most notably, depending on the optimization objective, only additional circuit models have to be derived and embedded within the split-circuit. The adjoint (dual) split-circuit models for the most prominent power flow components are derived in Section III.

Importantly, the corresponding equivalent circuit problems for the original and adjoint systems are solved using an extension of the recently introduced circuit simulation-based power flow methods described in [5],[6]. By utilizing specific variable constraints and applying a unique form of homotopy as needed, the circuit model-based formulation and solution can be used to ensure robust convergence and scalability to large problem sizes. This is in contrast with the aforementioned traditional approaches based on power mismatch equations that are known to struggle with convergence and scalability issues [14]. Several results are presented to validate the proposed approach in Sections VI. and VII.

II. POWER FLOW EQUIVALENT SPLIT-CIRCUIT FORMULATION

Modeling the power flow problem in terms of current and voltage state variables was demonstrated to provide a generalized framework for robust and efficient power grid steady-state analyses [3]-[6]. In this section, we briefly discuss the concept of the split-circuit modeling approach by showing the direct mapping for some of the most prominent power flow models to their split-circuit equivalents. Detailed derivations of the presented and other power-flow split circuit models can be found in [3]-[4],[9],[19].

The traditional ‘PQV’ formulation is an inherently non-linear formulation due to the power mismatch equations that define the network constraints. Though the network constraints are linear in the equivalent circuit formulation, nonlinearities are introduced by modeling the constant power behavior of power flow generator and load models [3]-[4]. Moreover, *due to the non-analyticity of the complex conjugate operator within the constant power models, the function has to be split into real and imaginary components in order to facilitate the use of the Newton-Raphson (NR) method to obtain the operating point of the power flow circuit.* As a consequence, the complete circuit has to be split into its real and imaginary components and coupled with controlled sources that map to the split complex circuit equations.

A. Transmission Line π -model

Consider a series element of a transmission line π model connecting buses k and m . Its complex governing circuit equation can be obtained from Ohm’s Law in terms of the series line impedance ($R_s + jX_s$) and the voltage across it (\tilde{V}_{km}) as:

$$\tilde{I}_{km} = (G_L + jB_L)\tilde{V}_{km} \quad (1)$$

$$\text{where } G_L + jB_L = \frac{R_s}{R_s^2 + X_s^2} - j\frac{X_s}{R_s^2 + X_s^2}.$$

We obtain the split-circuit governing equations by further splitting complex current from (1) into its real and imaginary components (I_{km}^R and I_{km}^I):

$$I_{km}^R = G_L V_{km}^R - B_L V_{km}^I \quad (2)$$

$$I_{km}^I = G_L V_{km}^I + B_L V_{km}^R \quad (3)$$

Terms from (2)-(3), where the real and imaginary current terms are respectively proportional to real and imaginary voltages (V_{km}^R and V_{km}^I), are mapped to a conductance, while the current terms proportional to the voltage across the other circuit represent voltage-controlled current sources. After applying the same approach to map the shunt parts of π model into its split-circuit equivalent [3], the complete transmission line power flow split-circuit can be obtained as shown in Fig. 1.

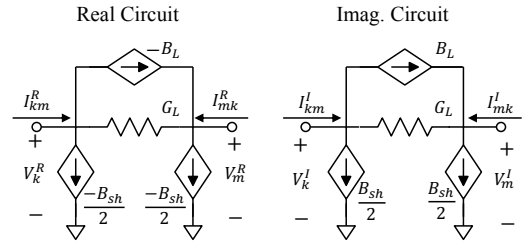


Fig. 1. Power flow split-circuit of a transmission line π -model.

B. Slack generator

The slack generator bus is defined by its voltage magnitude (V_{sb}) and angle (θ_{ref}). This model further sets the reference voltage angle and supplies the additional power needed for the pre-set generation power to meet the demand and line losses. In the equivalent split-circuit formulation, a slack bus generator is represented by an independent voltage source [19] in both real and imaginary circuits whose values are defined as:

$$V_{sb}^R = V_{sb} \cos \theta_{ref} \quad (4)$$

$$V_{sb}^I = V_{sb} \sin \theta_{ref} \quad (5)$$

C. Modeling nonlinear constant power models

The constant power-based PV and PQ circuit models are obtained from the definition of complex power in terms of the current that absorbs the constrained real (P_C) and reactive (Q_C) load powers at a bus voltage ($\tilde{V}_C = V_{RC} + jV_{IC}$) as:

$$\tilde{I}_C = \frac{P_C - jQ_C}{\tilde{V}_C^*} \quad (6)$$

To allow the application of NR, we split the complex current (\tilde{I}_C) from (6) to its real and imaginary components (I_{RC} and I_{IC}):

$$I_{RC} = \frac{P_C V_{RC} + Q_C V_{IC}}{V_{RC}^2 + V_{IC}^2} \quad (7)$$

$$I_{IC} = \frac{P_C V_{IC} - Q_C V_{RC}}{V_{RC}^2 + V_{IC}^2} \quad (8)$$

Since the PQ load constrains both real and reactive powers, its equivalent split-circuit model [3] is defined in terms of real and imaginary load currents (I_{RL} and I_{IL}) linearized by the first order Taylor expansion for $(k+1)^{th}$ iteration:

$$I_{RL}^{k+1} = \alpha_R^k + \frac{\partial I_{RL}^k}{\partial V_{RL}} V_{RL}^{k+1} + \frac{\partial I_{RL}^k}{\partial V_{IL}} V_{IL}^{k+1} \quad (9)$$

$$I_{IL}^{k+1} = \alpha_I^k + \frac{\partial I_{IL}^k}{\partial V_{RL}} V_{RL}^{k+1} + \frac{\partial I_{IL}^k}{\partial V_{IL}} V_{IL}^{k+1} \quad (10)$$

The current sensitivities from (9) and (10) that relate real and imaginary currents to the voltage across them (V_{RL} , V_{IL}) represent a conductance, while the sensitivities that are proportional to the voltage of other circuit are mapped to voltage controlled current sources. Lastly, the known legacy terms (α_R^k and α_I^k) are mapped to independent current sources, as shown in Fig. 2.

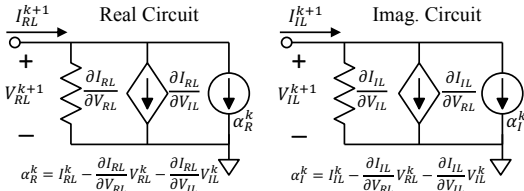


Fig. 2. Linearized power flow split-circuit of a PQ load.

In contrast to the slack bus generator whose powers are not bounded, the PV generator has a pre-set real power (P_G), and further adjusts its reactive power (Q_G) in order to control the bus voltage magnitude (V_{set}) [3]. It should be noted that the reactive power Q_G represents the added state variable in order to control the bus voltage magnitude, hence an additional constraint that relates real and imaginary voltages across the generator (V_{RG} , V_{IG}) has to be added:

$$F_G \equiv V_{RG}^2 + V_{IG}^2 - V_{set}^2 = 0 \quad (11)$$

Therefore, in addition to the voltage sensitivities, the current sensitivities with respect to reactive power are added in the linearized split-circuit model [3] as shown in Fig. 3. Furthermore, the nonlinearities from (11) are linearized by the first order Taylor expansion and stamped (values are added to the Jacobian in a modular way) to the system of circuit equations for additional Q_G variable within the formulation.:

$$2V_{RG}^k V_{RG}^{k+1} + 2V_{IG}^k V_{IG}^{k+1} = V_{RG}^{k+1}{}^2 + V_{IG}^{k+1}{}^2 + V_{set}^2 \quad (12)$$

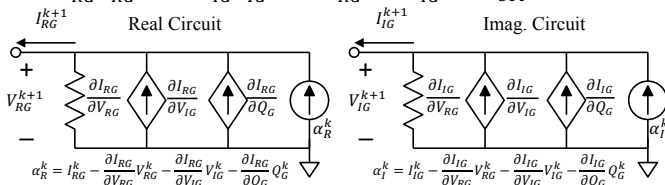


Fig. 3. Linearized power flow split-circuit of a PV generator.

Finally, after the equivalent split-circuit models for each of the power flow elements are built, they can be hierarchically combined to build the complete linearized equivalent circuit that is iteratively solved until convergence.

III. ADJOINT POWER FLOW EQUIVALENT SPLIT-CIRCUIT

The adjoint network concept introduced in [21]-[22] is a well-studied and understood concept that has been used for various circuit analyses, most notably noise analysis in SPICE [7]. It is

usually derived from Tellegen's Theorem and calculus of variations [20]. In the first part of this section, we provide a brief introduction to the adjoint network concept and further apply it to the linear network elements of our power flow equivalent circuit. Importantly, the adjoint circuit methodology is not developed for nonlinear steady-state elements defined at fixed frequency (models that constrain the complex power), hence we will further extend the adjoint network theory to derive the adjoint circuit models of nonlinear constant power elements within the power flow circuit formulation.

A. Adjoint equivalent of linear power flow split-circuits

Consider a linear time-invariant network \mathcal{N} and its topologically equivalent adjoint $\tilde{\mathcal{N}}$, where \tilde{I} , \tilde{V} , $\tilde{\mathfrak{I}}$ and $\tilde{\lambda}$ represent the network and adjoint branch current and voltage phasors respectively. From Tellegen's Theorem we can write the following relationship that has to be satisfied [20]-[22]:

$$\tilde{I}^T \tilde{\lambda} - \tilde{\mathfrak{I}}^T \tilde{V} = 0 \quad (13)$$

Next, if the circuit equations of network \mathcal{N} have a form of:

$$\tilde{I} = Y \tilde{V} \quad (14)$$

By substituting (14) in (13) we can obtain:

$$\tilde{V}^T (Y^H \tilde{\lambda}) = \tilde{V}^T \tilde{\mathfrak{I}} \quad (15)$$

Hence in order for Tellegen's Theorem to remain satisfied, the adjoint current $\tilde{\mathfrak{I}}$ that further defines the transformation from network \mathcal{N} to its adjoint $\tilde{\mathcal{N}}$ has to be equivalent to:

$$\tilde{\mathfrak{I}} = Y^H \tilde{\lambda} \quad (16)$$

As it can be seen from (16), the linear sensitivity (admittance) matrix of the adjoint circuit corresponds to the Hermitian of the original admittance matrix. Furthermore, since independent voltage and current sources are constant, their sensitivities are zero and, therefore, represent an open and short, respectively, in the adjoint domain [21]. In the following, the generalized mapping of linear circuit elements that represent the building blocks of linear power flow split-circuits (transmission line, shunt, slack bus, transformer, etc.) are presented in Table I.

TABLE I. MAPPING THE LINEAR POWER FLOW CIRCUIT TO DUAL DOMAIN

Powerflow circuit		Adjoint Powerflow circuit
Independent current source	→	open
Independent voltage source	→	short
Capacitor	→	Inductor
Inductor	→	Capacitor
Conductance	→	Conductance

1) Adjoint split-circuit of transmission line π -model

For the given line impedance ($R_s + jX_s$) and shunt susceptance (B_{sh}) of a transmission line model, we obtain its adjoint power flow circuit equations by using the relation defined in (16). The complex governing equation for the series part is given by Ohm's Law that relates the complex adjoint circuit current ($\tilde{\mathfrak{I}}_{km} = \mathfrak{I}_{km}^R + j\mathfrak{I}_{km}^I$) and voltage ($\tilde{\lambda}_{km} = \lambda_{km}^R + j\lambda_{km}^I$) as:

$$\tilde{\mathfrak{I}}_{km} = (G_L - jB_L) \tilde{\lambda}_{km} \quad (17)$$

The corresponding real and imaginary adjoint currents of a series elements are further obtained by splitting (17):

$$\mathfrak{I}_{km}^R = G_L \lambda_{km}^R + B_L \lambda_{km}^I \quad (18)$$

$$\mathfrak{I}_{km}^I = G_L \lambda_{km}^I - B_L \lambda_{km}^R \quad (19)$$

As in the case of mapping the power flow circuit, the terms where the adjoint current is proportional to the adjoint voltage drop across the line are modeled by conductance, while the other terms proportional to the voltage drop of the other adjoint circuit represent voltage-controlled current sources.

Similarly, the complex current flowing through the shunt element ($\mathfrak{I}_{k,sh}^R + j\mathfrak{I}_{k,sh}^I$) can be defined from (16) as in (20), which is further represented as voltage-controlled current sources in the adjoint circuit domain.

$$\mathfrak{I}_{k,sh}^R + j\mathfrak{I}_{k,sh}^I = \frac{B_{sh}}{2}\lambda_k^I - j\frac{B_{sh}}{2}\lambda_k^R \quad (20)$$

Finally, by combining the series and shunt split-circuits we obtain the complete adjoint power flow split-circuit of a transmission line as shown in Fig. 4.

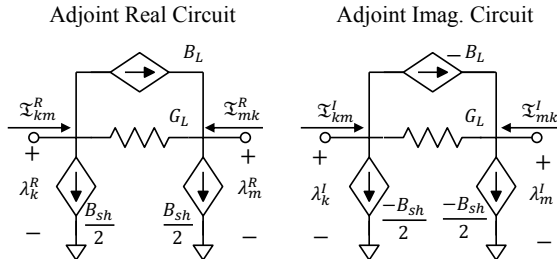


Fig. 4. Adjoint power flow split-circuit of a transmission line π -model.

2) Adjoint split-circuit of a slack generator

As the slack bus is modeled as an independent voltage source in both the real and imaginary circuits, the sensitivities are zero. Therefore, a zero-voltage source (short to ground) is used to represent the slack bus in both the real and imaginary adjoint equivalent circuits.

B. Adjoint equivalent of nonlinear power flow split-circuits

Nonlinear steady-state analysis for a fixed frequency point is not well explored in the circuit simulation field due to the lack of models that exhibit such behavior. Therefore, in order to derive the adjoint split-circuit models of nonlinear power flow elements (PV generator, PQ load), we extend the linear adjoint circuit methodology discussed in III.A.

Consider the split-circuit equations that govern the nonlinear power flow elements, expressed in terms of their first order sensitivities ($\mathcal{J}(V)$):

$$I_{NL} = \mathcal{J}(V)V + \gamma_{NL} \quad (21)$$

where I_{NL} , V and γ_{NL} represent the nonlinear split-circuit currents (I_R, I_I), state variables, and independent sources, respectively.

Since the independent sources γ_{NL} do not contribute to the adjoint circuit, they can be omitted in further derivations without loss of generality. Next, we substitute (21) into the generalized relationship obtained from Tellegen's Theorem in (13) to obtain the expression for the nonlinear adjoint current that further defines the transformation from power flow to the adjoint split-circuit:

$$\mathfrak{I}_{NL} = \mathcal{J}(V)^T \lambda \quad (22)$$

Note that if the sensitivity matrix $\mathcal{J}(V)^T$ is linear, (22) becomes equivalent to the split-circuit form of (16). Otherwise, the nonlinear elements from power flow also introduce nonlinearities within the adjoint power flow circuit.

1) Adjoint split-circuit of a PQ load

We start the derivation of the adjoint split-circuit of a PQ load by rewriting the power flow split-circuit governing equations from (9)-(10) in the form given in (21).

$$\begin{bmatrix} I_{RL} \\ I_{IL} \end{bmatrix} = \begin{bmatrix} \frac{\partial I_{RL}}{\partial V_{RL}} & \frac{\partial I_{RL}}{\partial V_{IL}} \\ \frac{\partial I_{IL}}{\partial V_{RL}} & \frac{\partial I_{IL}}{\partial V_{IL}} \end{bmatrix} \begin{bmatrix} V_{RL} \\ V_{IL} \end{bmatrix} + \begin{bmatrix} \alpha_{RL} \\ \alpha_{IL} \end{bmatrix} \quad (23)$$

The nonlinear adjoint circuit equations that define the PQ load can be further obtained from (22) as:

$$\begin{bmatrix} \mathfrak{I}_{RL} \\ \mathfrak{I}_{IL} \end{bmatrix} = \begin{bmatrix} \frac{\partial I_{RL}}{\partial V_{RL}} & \frac{\partial I_{RL}}{\partial V_{IL}} \\ \frac{\partial I_{IL}}{\partial V_{RL}} & \frac{\partial I_{IL}}{\partial V_{IL}} \end{bmatrix} \begin{bmatrix} \lambda_{RL} \\ \lambda_{IL} \end{bmatrix} \quad (24)$$

Further, since the current sensitivities from (24) represent the nonlinear functions of real and imaginary power flow voltages, we further linearize the nonlinear adjoint load currents using the first order Taylor expansion:

$$\begin{aligned} \mathfrak{I}_{RL}^{k+1} = & \beta_R^k + \frac{\partial \mathfrak{I}_{RL}^k}{\partial V_{RL}} V_{RL}^{k+1} + \frac{\partial \mathfrak{I}_{RL}^k}{\partial V_{IL}} V_{IL}^{k+1} + \frac{\partial \mathfrak{I}_{RL}^k}{\partial \lambda_{RL}} \lambda_{RL}^{k+1} \\ & + \frac{\partial \mathfrak{I}_{RL}^k}{\partial \lambda_{IL}} \lambda_{IL}^{k+1} \end{aligned} \quad (25)$$

$$\begin{aligned} \mathfrak{I}_{IL}^{k+1} = & \beta_I^k + \frac{\partial \mathfrak{I}_{IL}^k}{\partial V_{RL}} V_{RL}^{k+1} + \frac{\partial \mathfrak{I}_{IL}^k}{\partial V_{IL}} V_{IL}^{k+1} + \frac{\partial \mathfrak{I}_{IL}^k}{\partial \lambda_{RL}} \lambda_{RL}^{k+1} \\ & + \frac{\partial \mathfrak{I}_{IL}^k}{\partial \lambda_{IL}} \lambda_{IL}^{k+1} \end{aligned} \quad (26)$$

Lastly, (25)-(26) are mapped to an equivalent circuit, where the current terms that are proportional to the adjoint voltage across the load terminals represent conductances, and the terms related to the voltages in the opposite sub-circuit define controlled-current sources. Historical terms known from the previous iteration are given by independent current sources.

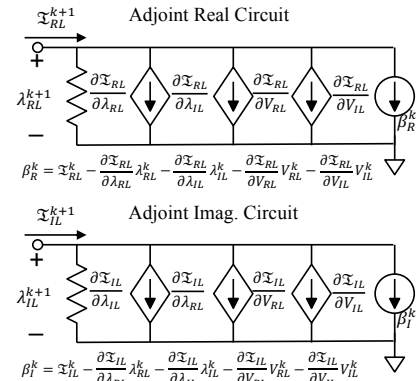


Fig. 5. Linearized adjoint power flow split-circuit of a PQ load.

2) Adjoint split-circuit of a PV generator

The governing power flow split-circuit equations of a PV generator can be expressed in the form defined by (21) as:

$$\begin{bmatrix} I_{RG} \\ I_{IG} \\ 0 \end{bmatrix} = \begin{bmatrix} \frac{\partial I_{RG}}{\partial V_{RG}} & \frac{\partial I_{RG}}{\partial V_{IG}} & \frac{\partial I_{RG}}{\partial Q_G} \\ \frac{\partial I_{IG}}{\partial V_{RG}} & \frac{\partial I_{IG}}{\partial V_{IG}} & \frac{\partial I_{IG}}{\partial Q_G} \\ \frac{\partial F_G}{\partial V_{RG}} & \frac{\partial F_G}{\partial V_{IG}} & 0 \end{bmatrix} \begin{bmatrix} V_{RG} \\ V_{IG} \\ Q_G \end{bmatrix} + \begin{bmatrix} \alpha_{RG} \\ \alpha_{IG} \\ f_G \end{bmatrix} \quad (27)$$

The nonlinear adjoint circuit of a PV generator can be then obtained by applying the transformation from (22):

$$\begin{bmatrix} \mathfrak{I}_{RG} \\ \mathfrak{I}_{IG} \\ 0 \end{bmatrix} = \begin{bmatrix} \frac{\partial I_{RG}}{\partial V_{RG}} & \frac{\partial I_{IG}}{\partial V_{RG}} & \frac{\partial F_G}{\partial V_{RG}} \\ \frac{\partial I_{RG}}{\partial V_{IG}} & \frac{\partial I_{IG}}{\partial V_{IG}} & \frac{\partial F_G}{\partial V_{IG}} \\ \frac{\partial I_{RG}}{\partial Q_G} & \frac{\partial I_{IG}}{\partial Q_G} & 0 \end{bmatrix} \begin{bmatrix} \lambda_{RG} \\ \lambda_{IG} \\ \lambda_Q \end{bmatrix} \quad (28)$$

As in the case of the nonlinear adjoint PQ load, the first two equations from (28) represent the nonlinear real and imaginary adjoint generator currents. These can be linearized by a first order Taylor expansion to define the adjoint split-circuit as shown in Fig. 6. The third equation represents the adjoint equivalent of the voltage magnitude constraint from the power flow circuit and can be simplified as:

$$V_{IG}\lambda_{RG} - V_{RG}\lambda_{IG} = 0 \quad (29)$$

It can be shown that the relationship between power flow and adjoint bus voltages from (29) constrains the PV bus voltage angle of the adjoint circuit to be equal to the respective voltage angle of the power flow circuit. Lastly, (29) is linearized and stamped for the λ_Q adjoint variable as in the case of the voltage magnitude constraint.

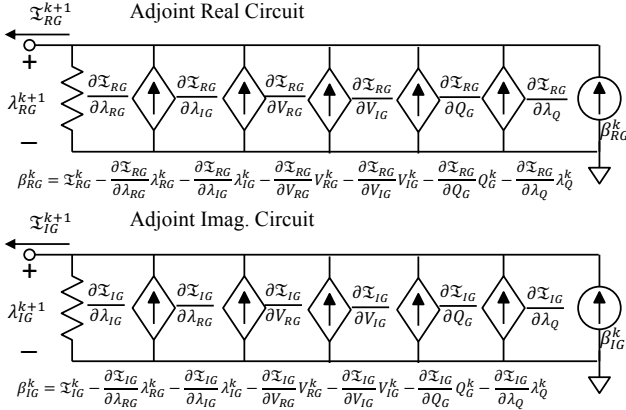


Fig. 6. Linearized adjoint power flow split-circuit of a PV generator.

C. Infeasibility current source

It is important to note that since the slack bus model represents a short circuit in the adjoint domain, the adjoint power flow circuit does not have a source to set its operating point. Therefore, it can be shown that if a power flow solution exists, the adjoint circuit has a feasible and trivial solution, i.e. zero voltage at all nodes. In contrast, the operating point of the adjoint circuit is undefined when the power flow solution is infeasible. Hence, introduction of an additional current source at a power flow circuit node that is controlled by a corresponding adjoint voltage does not affect the solution of the power flow circuit if a feasible point exists. However, when the system is infeasible, the additional source will “pick up the slack” and prevent KCL violations at the corresponding node by using it to set an operating point of the adjoint circuit. The non-zero voltages in the adjoint circuit now indicate the nodes where KCL cannot be satisfied in the original system.

Herein, we introduce the infeasibility current source model, which couples the power flow circuit to its adjoint circuit, thereby ensuring feasibility of the coupled simulation problem.

In order to distinguish between these new controlled sources and the ones used in our split equivalent circuit formulation for power flow, we represent the infeasibility sources as in Fig. 7.

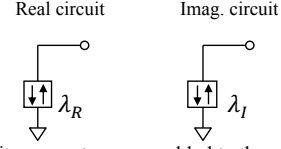


Fig. 7. Infeasibility current sources added to the power flow circuit.

D. Optimality of Adjoint Power Flow Analysis

Herein, we demonstrate the relationship between the proposed Adjoint Power Flow Analysis and the optimization problem of minimizing the L2-norm of the current sources (I_F) that are connected to each node of the power flow circuit, excluding the voltage magnitude control equations.

First, consider the generalized form of circuit equations that represent the power flow and its adjoint circuits coupled through the feasibility currents, namely (14), (21)-(22):

$$\begin{bmatrix} Y_{GB} + J(V^k) & -\hat{\mathbf{1}} \\ \frac{\partial J^T(V^k)}{\partial V} & Y_{GB}^T + J^T(V^k) \end{bmatrix} \begin{bmatrix} V \\ \lambda \end{bmatrix} = \begin{bmatrix} \alpha \\ \beta \end{bmatrix} \quad (30)$$

where Y_{GB} represents the linear admittance matrix from (14), defined for the split-circuit models and $\hat{\mathbf{1}}$ is a degenerate identity matrix with zero diagonal entries corresponding to the indices of voltage magnitude constraints.

Next, in order to show how the set of circuit equations from (30), relates to the optimality conditions of an optimization problem, we define the following program:

$$\min_{I_F} \frac{1}{2} \|I_F\|_2^2 \quad (31)$$

Subject to power flow constraints with additional currents:

$$Y_{GB}V + J(V)V = I_F + \alpha \quad (32)$$

To find the optimality conditions of the optimization problem defined by (31)-(32), we define the Lagrangian function as:

$$\mathcal{L}(V, I_F, \lambda) = \frac{1}{2} \|I_F\|_2^2 + \lambda^T (Y_{GB}V + J(V)V - \alpha - I_F) \quad (33)$$

The necessary KKT optimality conditions are further obtained by differentiating (33) with respect to power flow and adjoint variables, as well as newly introduced current (I_F) variables:

$$\frac{\partial \mathcal{L}}{\partial V} \rightarrow [Y_{GB}^T + J^T(V)]\lambda = 0 \quad (34)$$

$$\frac{\partial \mathcal{L}}{\partial I_F} \rightarrow I_F = \lambda \quad (35)$$

$$\frac{\partial \mathcal{L}}{\partial \lambda} \rightarrow [Y_{GB} + J(V)]V - I_F = \alpha \quad (36)$$

After linearizing (34) and eliminating the (I_F) variables by substituting (35) in (36), we end up with the system of equations from (30). From this we postulate the following theorem.

Theorem 1. Let \mathcal{N} and its topologically equivalent adjoint $\tilde{\mathcal{N}}$ represent the power flow and adjoint power flow circuits respectively, that are further coupled through infeasibility current sources connected to every node of the power flow circuit \mathcal{N} . Then, the solution of the two fully coupled split-circuits represents the operating point that provides minimal current flow between the power flow circuit and its adjoint; i.e. the infeasibility currents are minimized.

Proof. Following from (30) and (34)-(36), the governing circuit equations of the Adjoint Power Flow problem represent the necessary KKT optimality conditions of the optimization problem given by (31)-(32). Additionally, since the constant power-based models introduce the nonlinearities within the equivalent circuit, let V^* represent an obtained equivalent circuit operating point that satisfies the second order KKT sufficient condition as:

$$\tau^T \frac{\partial \mathcal{J}^T(V^*)}{\partial V} \tau > 0 \quad \forall (\tau \neq \mathbf{0}) \in T_{V^*} \quad (37)$$

where T_{V^*} represents the tangent linear sub-space at V^* [23].

Then, the operating point of the proposed Adjoint Power Flow equivalent circuit problem represents an optimal solution that in addition to locating the source of infeasibility for the simulation model, optimally allocates (minimizes) the current violations used to set the operating point of the adjoint circuit through the infeasibility current sources. ■

From the perspective of the optimization problem, the infeasibility current sources do not have to be added to the voltage magnitude constraints, since by Ohm's Law and KCL there is always a current that can be injected into the node of power flow circuit that prevents the system solution from being infeasible. *This further eliminates the need for multi-objective optimization and additional weighting factors that have to be assigned in order to obtain the physically meaningful optimal solution*, as required by other proposed approaches to determine the power flow infeasibility [14]. Importantly, the solution of the adjoint power flow problem still depends on the initial power flow starting point, that if projected to the adjoint space preserves the power flow convergence properties. This is further validated for a generated test case library and presented in Section VI.

IV. BUILDING AND SOLVING AN EQUIVALENT SPLIT-CIRCUIT

A. Generalized power system problem

An equivalent split-circuit formulation was demonstrated to provide a generalized power system simulation framework [3]-[6], [24]-[25] that can include any physics-based model, such as induction motors [9] or power electronic devices [24]. Since both transmission and distribution networks can be represented by an equivalent circuit, they can be simulated (jointly [6] or separately [25]) within the same framework.

As it is shown in the previous sections, each of the power system split-circuit device models (PV generator, PQ load, etc.) can be further defined within the adjoint (dual) domain. The complete split-circuit representation is then obtained by hierarchically combining (connecting) the derived power flow and adjoint power flow circuit models, as defined by the grid (network) topology. It is important to note that the hierarchical building of the circuit representation corresponds to a modular construction of the Jacobian/Hessian matrix and constant vector that defines the Newton (Raphson) values during the iteration process.

Coupling the power flow with its adjoint circuit corresponds to solving an optimization problem whose objective is specified by the type of coupling between the two circuits. *This further defines a new class of the optimization problems, Equivalent Circuit Programming (ECP), whose constraints can be*

expressed in terms of equivalent circuit equations, and whose solutions can therefore be obtained by solving circuit simulation problems. As shown for the proposed Adjoint-enhanced Power Flow analysis, coupling the power flow circuit with its adjoint through the infeasibility (adjoint) sources optimally captures the problem infeasibility. Adding the adjoint sources to the power flow circuit to capture infeasibility can be done in the beginning of the simulation, where simulating the circuit corresponds to solving an optimization problem, or during the power flow simulation, when the iterative simulation method starts diverging, thereby indicating possible infeasibility.

B. Generalized solution of an equivalent split-circuit

Once the complete equivalent split-circuit is built, its set of governing circuit equations correspond to the nonlinear set of equations as linearized by a first order Taylor expansion. This linearization represents that for the inner most loop of the Newton (Raphson) method. Iteratively solving the circuit simulation problem corresponds to Newton (Raphson) iterations, where at every iteration only circuit elements (Jacobian/Hessian terms) that are dependent on the values from the previous iteration are rebuilt, while the linear parts are only built once at the beginning of the simulation. This approach was shown to represent an extremely efficient formulation and solution method for solving the nonlinear circuit problems [8],[20]. The main difference between the circuit simulation and traditional Newton (Raphson) method, however, is the circuit formalism obtained from the circuit representation of the problem. This provides important information that allows for developing efficient heuristics for limiting the Newton step, thereby ensuring stable and efficient convergence properties [3]-[6],[8]. This is further discussed in Section V.

Initialization of the power flow split-circuit is well defined by the power flow problem as it is specified [3]-[6]. When initializing the adjoint power flow circuit, we need to consider that the adjoint voltages also correspond to the magnitude of infeasibility currents in the power flow analysis at the value buses. Hence, we initialize them to a small constant value such as the NR tolerance used for the convergence criterion. After the circuit initialization and first iteration, the linearized circuit elements are updated as discussed in Section V.

To clarify the proposed framework, we provide a simple 2-bus network example and work through the steps from building to iteratively solving an equivalent circuit in order to obtain the optimal solution.

C. Example: Adjoint Power Flow analysis

Let us consider a simple 2-bus network example consisting of a slack bus connected to a PQ load, as shown in Fig. 8.

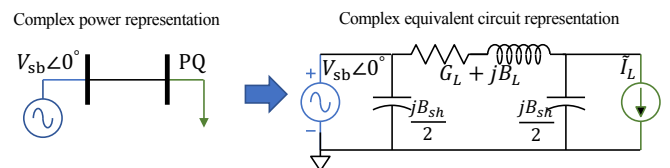


Fig. 8. PQV and equivalent circuit representations of a 2-bus network.

By writing the governing KCL equations of the 2-bus network from Fig. 8, we can show that the nodal equation corresponding

to the load bus contains the nonlinear term defined by the complex conjugate operator:

$$\frac{P - jQ}{\tilde{V}_L^*} + \frac{jB_{sh}}{2} \tilde{V}_L + (G_L + jB_L)(\tilde{V}_L - \tilde{V}_{sb}) = 0 \quad (38)$$

Thus, derivative-based iterative methods such as Newton-Raphson cannot be directly applied. We then split the complex equations into its real and imaginary parts [3]-[6] that corresponds to the split-circuit in Fig. 9.

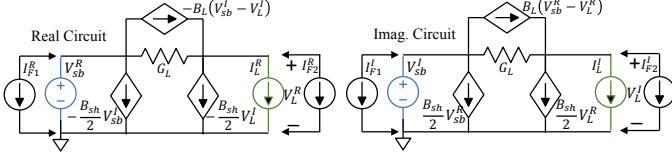


Fig. 9. Nonlinear split-circuit of a 2-bus network. PQ load currents as given by (7)-(8) introduce the circuit nonlinearities.

The proposed Adjoint Power Flow problem can be solved by adding current sources to each node of the nonlinear split-circuit from Fig. 9, and plugging the underlying circuit equations into one of the commercial toolboxes. Instead, we hierarchically build the linearized split-circuit by combining the previously derived split-circuit models, and iteratively solve it while applying circuit simulation techniques to ensure robust and efficient convergence. Since the example consists of a slack bus and a PQ load connected through a pi-segment of a slack bus, transmission line (Fig. 1 and Fig. 4), a PQ load (Fig. 2 and Fig. 5), and feasibility sources, derived in Section III, and connect them together to form the circuit shown in Fig. 10.

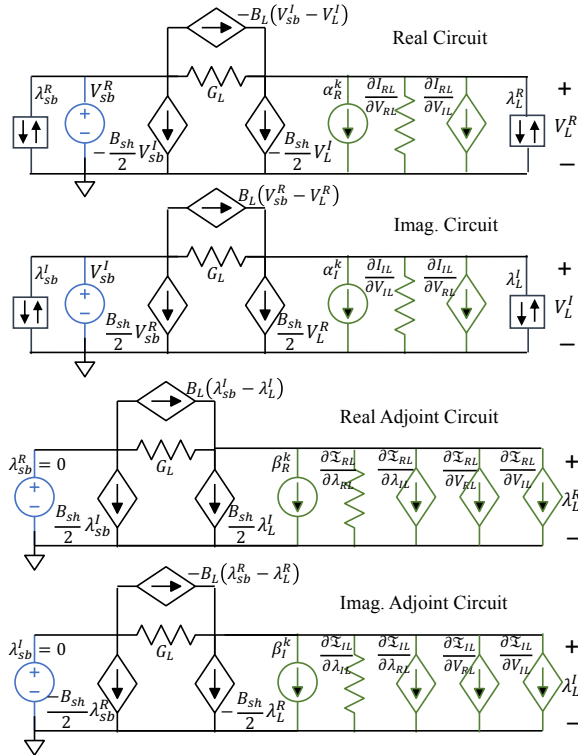


Fig. 10. Equivalent split-circuit of the 2-bus power flow feasibility problem.

Building the equivalent split-circuit from Fig. 10 corresponds to building the linearized system of equations. For instance, the terms of the generalized circuit equations defined in (30) that correspond to the 2-bus case from Fig. 10 are given as:

$$Y_{GB} = \begin{bmatrix} 1 & 0 & G_L & -B_L - \frac{B_{sh}}{2} & -G_L & B_L \\ 0 & 1 & B_L + \frac{B_{sh}}{2} & G_L & -B_L & -G_L \\ 0 & 0 & -G_L & B_L & G_L & -B_L - \frac{B_{sh}}{2} \\ 0 & 0 & -B_L & -G_L & B_L + \frac{B_{sh}}{2} & G_L \\ 0 & 0 & 1 & 0 & 0 & 0 \\ 0 & 0 & 0 & 1 & 0 & 0 \end{bmatrix} \quad (39)$$

$$J(V^k) = \begin{bmatrix} 0 & 0 & 0 & 0 & 0 & 0 \\ 0 & 0 & 0 & 0 & 0 & 0 \\ 0 & 0 & 0 & 0 & \frac{\partial I_{RL}^k}{\partial V_{RL}} & \frac{\partial I_{RL}^k}{\partial V_{IL}} \\ 0 & 0 & 0 & 0 & \frac{\partial I_{IL}^k}{\partial V_{RL}} & \frac{\partial I_{IL}^k}{\partial V_{IL}} \\ 0 & 0 & 0 & 0 & 0 & 0 \\ 0 & 0 & 0 & 0 & 0 & 0 \end{bmatrix}, \alpha = \begin{bmatrix} 0 \\ 0 \\ -\alpha_{RL}^k \\ -\alpha_{IL}^k \\ V_{sb}^R \\ V_{sb}^I \end{bmatrix} \quad (40)$$

$$\frac{\partial J^T(V^k)}{\partial V} = \begin{bmatrix} 0 & 0 & 0 & 0 & 0 & 0 \\ 0 & 0 & 0 & 0 & 0 & 0 \\ 0 & 0 & 0 & 0 & \frac{\partial \mathfrak{I}_{RL}^k}{\partial V_{RL}} & \frac{\partial \mathfrak{I}_{RL}^k}{\partial V_{IL}} \\ 0 & 0 & 0 & 0 & \frac{\partial \mathfrak{I}_{IL}^k}{\partial V_{RL}} & \frac{\partial \mathfrak{I}_{IL}^k}{\partial V_{IL}} \\ 0 & 0 & 0 & 0 & 0 & 0 \\ 0 & 0 & 0 & 0 & 0 & 0 \end{bmatrix}, \beta = \begin{bmatrix} 0 \\ 0 \\ -\beta_{RL}^k \\ -\beta_{IL}^k \\ 0 \\ 0 \end{bmatrix} \quad (41)$$

V. EXTENDING THE CIRCUIT SIMULATION METHODS

The circuit formalism was demonstrated to provide understanding of the characteristics of each power flow state variable and its sensitivities directly from first principles. As it was shown in [4]-[6], during the solution process of a power flow problem, a large NR step may lead the solution trajectory out of a well-defined solution space and result in either divergence or convergence to a non-physical solution. It is, therefore, crucial to limit the NR step before it makes an invalid step out of the solution space. Furthermore, limiting methods may fail to converge for large-scale ill-conditioned test cases solved from an arbitrary initial guess. Hence, the use of homotopy methods, such as ‘‘Tx-stepping’’ in [5], is crucial to ensure convergence. Importantly, the nonlinearities of the adjoint split-circuit resemble the ones already robustly handled within the power flow problem, while the feasibility of the simulation problem is ensured. Thus, in this section we extend the recently introduced circuit simulation limiting and homotopy methods to ensure robust the convergence of any size power systems.

A. Voltage limiting

Voltage Limiting was shown to be a simple and effective simulation technique that limits the absolute value of the step change that the real and imaginary voltage vectors are allowed to make during each NR iteration [3]-[6]. The power flow voltage step limiting technique is given in compact form as:

$$\xi_C = \min \left[1, \text{sign}(\Delta V_C^k) \frac{\Delta V_{max}^k}{\Delta V_C^k} \right] \quad (42)$$

where a placeholder $C \in \{R, I\}$, ΔV_C^k and $\Delta \lambda_C^k$ represent the power flow and adjoint voltage NR steps, while ΔV_{max}^k is a maximum allowable step change.

The hard limit (V_{max}) is then imposed in order to prevent the voltage variables to escape the physical solution space:

$$\xi_C = \begin{cases} \min \left[\xi_C, \frac{V_{max} - V_C^k}{\Delta V_C^k} \right] : \forall \Delta V_C^k > 0 \\ \min \left[\xi_C, \frac{-V_{max} - V_C^k}{\Delta V_C^k} \right] : \forall \Delta V_C^k < 0 \end{cases} \quad (43)$$

Lastly, the obtained limiting factors are used to limit the step change of power flow and adjoint power flow voltages as:

$$\hat{V}_C^{k+1} = V_C^k + \xi_C \Delta V_C^k \quad (44)$$

$$\hat{\lambda}_C^{k+1} = \lambda_C^k + \xi_C \Delta \lambda_C^k \quad (45)$$

B. Tx-Stepping homotopy method

To allow the robust convergence of any large-scale power system simulation problem, we extend the recently introduced Tx-stepping method [5] to the adjoint power flow simulation.

The solution of the feasibility simulation problem (coupled power flow and adjoint power flow circuits), is obtained by embedding the homotopy factor $\mu \in [0,1]$ to linear series network elements and transformer model as shown in (46)-(48) and sequentially solving the relaxed feasibility problems while gradually decreasing the homotopy factor to zero. Namely, for the initial homotopy factor set to one, the circuit of the feasibility problem is virtually ‘‘shorted’’. Now, the power flow solution is feasible and driven by the generator voltages and the slack bus angle and can be trivially obtained. Gradual decreasing of the embedded homotopy factor μ to zero sequentially relaxes the feasibility circuit toward its original state, while using the solution from the previous sub-problem to initialize the feasibility circuit for the next homotopy decrement:

$$G_{km} + jB_{km} = (1 - \mu Y)(G_{km} + jB_{km}) \quad (46)$$

$$t(\mu) = t + (1 - t)\mu \quad (47)$$

$$\theta_{ph}(\mu) = (1 - \mu)\theta_{ph} \quad (48)$$

where Y represents an admittance scaling factor, t is the transformer tap, and θ_{ph} is the phase shifting angle.

Most importantly, any homotopy-embedded model defined for the adjoint circuit has to be governed by transformations given in (16) and (22). Therefore, transformer and phase shifter parameters remain scaled by (47)-(48) within their respective adjoint models, while the scaled homotopy admittance becomes conjugated, as shown in Fig. 11.

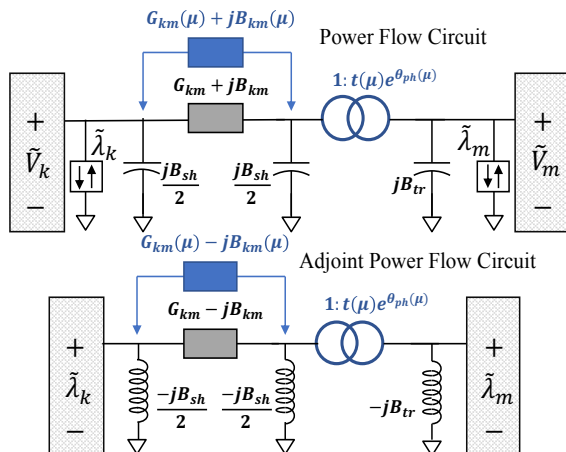


Fig. 11. Generic representation of Tx-stepping homotopy method.

VI. VALIDATING THE ADJOINT POWER FLOW ANALYSIS

The circuit element library for the introduced adjoint power flow models was built and incorporated within our prototype simulator Simulation with Unified Grid Analyses and Renewables (SUGAR). To validate the proposed adjoint power flow analysis for evaluating the feasibility, we demonstrate that its solution exactly matches the power flow solution, if such a solution exists. Therefore, we generate and examine the library with three different categories of test cases that are available in literature: 1. *Benchmark ill-conditioned test cases* [26]-[27], 2. *European RTE and PEGASE test cases* [28], 3. *Recently introduced synthetic USA test cases* [29].

Each of the test cases is run in SUGAR on a machine with an Intel Core i7-6700 3.4GHz processor. Table II shows the results of the analyses match exactly, indicating the Adjoint Power Flow analysis returns the same solution as regular power flow when the system is feasible.

TABLE II. VALIDATING ADJOINT POWER FLOW RESULTS IN FEASIBLE CASES

Test Case	Power Flow [3]-[6]				Adjoint Power Flow			
	V_{min}	V_{max}	θ_{min}	θ_{max}	V_{min}	V_{max}	θ_{min}	θ_{max}
case11_0.9982	0.795	1.174	-25.0	0.0	0.795	1.174	-25.0	0.0
case145	0.915	1.209	-73.9	29.0	0.915	1.209	-73.9	29.0
case1354pegase	0.981	1.108	-50.2	8.4	0.981	1.108	-50.2	8.4
case1888rte	0.847	1.101	-48.7	11.6	0.847	1.101	-48.7	11.6
case2869pegase	0.964	1.141	-60.8	55.3	0.964	1.141	-60.8	55.3
case6515rte	0.559	1.176	-72.5	13.0	0.559	1.176	-72.5	13.0
case9241pegase	0.789	1.156	-61.4	69.6	0.789	1.156	-61.4	69.6
WECC	0.946	1.081	-89.1	18.5	0.946	1.081	-89.1	18.5
case13659pegase	0.839	1.181	-34.7	98.6	0.839	1.181	-34.7	98.6
Eastern Inter.	0.938	1.090	-177.1	35.9	0.938	1.090	-177.1	35.9
Synthetic USA	0.904	1.090	-111.9	108.1	0.904	1.090	-111.9	108.1

The addition of the adjoint power flow split-circuit increases the size of the simulation problem. Therefore, in order to study the effect on the simulation runtime, we compare the average time per iteration of Power Flow and our Adjoint-enhanced Power Flow analysis in Fig. 12. As expected, there is an increase in average time per iteration. However, the trade-off between power flow divergence during infeasibility and simulation runtime for proposed adjoint power flow formulation can be justified by the ability to converge and optimally locate cases of power flow infeasibility. Most importantly, the simulation runtime is not significantly affected, which makes the proposed formulation a promising analysis for future implementations in contingency simulations.

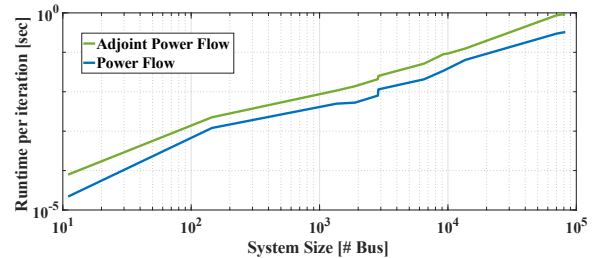


Fig. 12. Average runtime per iteration comparison

VII. SIMULATING AND LOCATING POWER FLOW INFEASIBILITY

After proving the optimality of the proposed adjoint power flow approach in Section III and validating the results for feasible power flow test cases in Section VI, we apply the proposed framework to examine and locate infeasibilities that may arise due to the operation at the edge of voltage collapse or a contingency.

1. Feasibility analysis of ill-conditioned 11 bus test case

The authors in [26] have demonstrated that the 11-bus distribution test case is genuinely ill-conditioned beyond a maximum loading factor of 99.82%. Hence, numerical error or the choice of convergence criterion can cause the difference between infeasibility (divergence of the numerical algorithm) or convergence to the feasible operating solution.

In this study, the adjoint power flow is solved for slight loading factor increments to locate and examine the appearance and evolution of infeasible regions within the test case. The simulation results representing the network topology for four different loading factors (three of which are provably infeasible) are presented in Fig. 13.

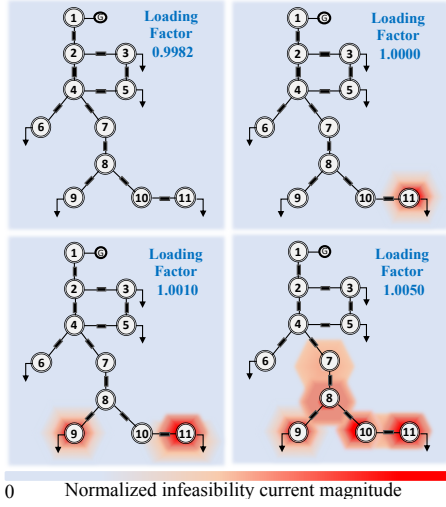


Fig. 13. Evaluating the feasibility of ill-conditioned 11 bus test case. The magnitude of infeasibility current is normalized with respect to the highest one encountered throughout the simulation of all four cases.

Referring to Fig. 13, after the known point of collapse is reached, the system first becomes infeasible (indicated by the heatmap around the infeasible bus) furthest from the slack generator (bus 11). As the loading factor keeps increasing, the infeasibility, which represents the amount of additional current needed to prevent the violation of KCL at each bus, evolves throughout the system.

To compare the proposed Adjoint Power Flow analysis with an existing formulation that minimizes infeasible real and reactive power injection within the power-mismatch formulation, we implemented the formulation from [14] in ‘SQP-FMINCON’ with the MATLAB optimization toolbox. The iteration count and infeasible p.u. real and reactive powers (P_{INF} and Q_{INF}) for two loading factors are shown in Table III.

TABLE III. RESULT COMPARISON FOR ILL-CONDITIONED 11 BUS CASE

Formulation	Loading factor: 1.0000		Loading factor: 1.1000	
	Iter. #	P_{INF} Q_{INF} [p.u.]	Iter. #	P_{INF} Q_{INF} [p.u.]
Adjoint Power Flow	16	3.179E-4 2.570E-4	14	0.0198 0.0157
PQ Formulation [14]	73	3.178E-4 2.572E-4	29	0.0198 0.0157

As expected, both formulations were able to converge to the same optimal infeasibility values. The proposed Adjoint Power Flow that was solved as a circuit simulation problem, however, converged to the optimal solution much faster, especially near the system collapse point where the power flow Jacobian is singular. This can be attributed to the efficient circuit simulation limiting heuristics that we apply in our simulation framework [3]-[6] for faster convergence.

2. Locating and correcting the infeasibility in a real-life N-1 contingency test case

Divergence of the power flow simulation during an N-1 analysis does not ensure problem infeasibility and hence does not provide complete information about the analyzed grid. In this example, we analyze a contingency test case of a real power system with over 5k buses that represents an N-1 contingency.

Solving the adjoint power flow problem provided information about the localized area that caused the infeasibility of the problem due to a reactive power deficiency, as shown in Fig. 14. By activating a continuous FACTS device near the infeasible region, we were able to restore the feasibility of the system.

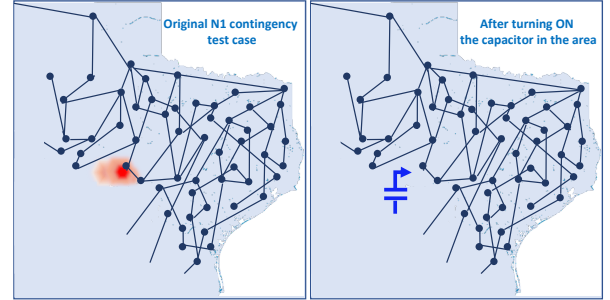


Fig. 14. Detecting and correcting the infeasibility on a real-life contingency case. Note that the network connectivity doesn't represent the true connectivity of the examined case.

3. Infeasibility of Synthetic USA grid test case during N-1 contingency analysis

The scalability of proposed adjoint power flow formulation is further tested by analyzing the feasibility of a recently developed test case representing the entire US grid, consisting of synthetic versions of the Eastern and Western Interconnections (WECC) as well as the ERCOT grid [29], during an N-1 contingency. The N-1 contingency we applied represented disconnecting the branch between buses 23510 (SENECA 7 1) and 23515 (SENECA 7 6). Adjoint power flow simulation results indicate this contingency represents an infeasible system, with the local area of infeasibility shown in Fig. 16. Note that the infeasible area information on the map represents an accurate location based on the synthetic test case; however, the graph does not correspond to the true connectivity of the US Grid.

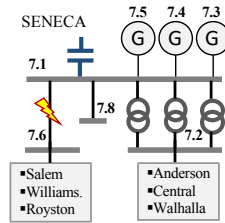


Fig. 15. Schematic representation of examined N1 contingency: removing the transmission line between buses SENECA 7.1 (23510) and SENECA 7.6 (23515) within the Oconee Nuclear station, near Seneca, SC

After analyzing the affected infeasible area and replacing the fixed shunt capacitor connected at the most infeasible bus (SENECA 7.1) with a continuous shunt device, the system becomes feasible again. Most importantly, as in the previous contingency test case, the detected infeasibilities were local and mostly due to reactive power deficiency. Further installation or activation of a reactive power compensating device in the area

was shown to restore the power flow feasibility. It should be noted that actual U.S. Eastern Interconnect testcases for N-1 contingencies were found to be significantly more resilient [5].

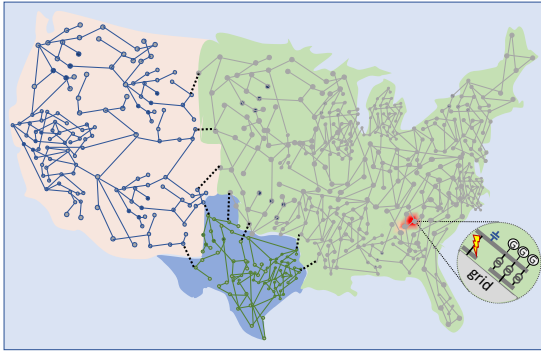


Fig. 16. Detecting infeasibility due to the contingency in synthetic test case representation of USA grid. Note that replacing the fixed shunt capacitor at bus 23515 (SENECA 7 1) with a variable capacitor restores the feasibility of the power flow problem

As shown by the simulation results, placement of infeasibility current sources within the power flow circuit can enable various analyses. For instance, the 11-bus test case presents the application toward optimal load shedding, while the real-life contingency test case optimally indicated the reactive power compensating device that has to be activated in order to restore feasibility of the network. Hence the respective placement of infeasibility current sources to all load buses and existing variable shunt devices will provide all the necessary information needed to analyze the feasibility of the simulation. Importantly, placing the infeasibility sources at nodes of critical infrastructure within the grid model can allow the optimal planning a new corrective device that would ensure N-1 contingency criteria required by NERC is met [30].

VIII. CONCLUSIONS

In this paper we introduced the adjoint power flow analysis for evaluating the feasibility of power flow cases as an extension of the recently introduced circuit theoretic approach for simulating the power flow problem. The infeasibility current sources and adjoint power flow split-circuit models are derived, and once coupled to the power flow circuit, shown to optimally prevent violation of KCL that arise for infeasible systems as a consequence of constant power models. Subsequently, recently proposed circuit simulation techniques are extended to ensure robust convergence properties of the adjoint power flow circuit. Finally, proposed framework was demonstrated to provide an efficient methodology for locating and evaluating power flow infeasibilities and can be further utilized to inform corrective actions in order to restore the feasibility of power flow problems.

IX. REFERENCES

- [1] Electric Power Research Institute. Application of advanced data processing, mathematical techniques and computing technologies in control centers: Enhancing speed and robustness of power flow computation, December 2012. Technical Update.
- [2] P. Kundur, N.J. Balu, and M.G. Lauby, "Power system stability and control". New York: McGraw-Hill, 1994, vol.7
- [3] M. Jereminov, D. M. Bromberg, L. Xin, G. Hug, L. Pileggi, "Improving Robustness and Modeling Generality for Power Flow Analysis," *T&D Conference and Exposition, 2016 IEEE PES*.
- [4] A. Pandey, M. Jereminov, G. Hug, L. Pileggi, "Improving Power Flow Robustness via Circuit Simulation Methods," *IEEE PES General Meeting*, Chicago, 2017.
- [5] A. Pandey, M. Jereminov, M. Wagner, G. Hug, L. Pileggi, "Robust Convergence of Power Flow using Tx Stepping Method with Equivalent Circuit Formulation" XX (PSCC), Dublin, Ireland, 2018.
- [6] A. Pandey, M. Jereminov, M. Wagner, D. M. Bromberg, G. Hug, L. Pileggi, "Robust Power Flow and Three Phase Power Flow Analyses", *IEEE Trans. on Power Systems*. DOI: 10.1109/TPWRS.2018.2863042
- [7] L. Nagel, R. Rohrer, "Computer Analysis of Nonlinear Circuits, Excluding Radiation (CANCER)", *IEEE Journal on Solid-State Circuits*, Vol. Sc-6, No.4, August 1971.
- [8] L. Pileggi, R. Rohrer, C. Visweswariah, *Electronic Circuit & System Simulation Methods*, McGraw-Hill, Inc., New York, NY, USA, 1995.
- [9] A. Pandey, M. Jereminov, X. Li, G. Hug, L. Pileggi, "Unified Power System Analyses and Models using Equivalent Circuit Formulation," *IEEE PES Innovative Smart Grid Technologies*, Minneapolis, USA, 2016.
- [10] T. Chen, D. Mehta, "On the Network Topology Dependent Solution Count of the Algebraic Load Flow Equations", *IEEE Trans. on Power Systems*, vol. 33-2, July 2017.
- [11] I. A. Hiskens, R. J. Davy, "Exploring the Power Flow Solution Space Boundary", *IEEE Trans. on Power Systems*, Vol. 16-3 August 2001.
- [12] C. Liu, C. Chang, J. A. Jiang and G. H. Yeh, "Toward a CPFLOW-based algorithm to compute all the type-1 load-flow solutions in electric power systems," in *IEEE Transactions on Circuits and Systems I: Regular Papers*, vol. 52, no. 3, pp. 625-630, March 2005.
- [13] D. K. Molzahn, V. Dawar, B. C. Lesieutre, C. DeMarco, "Sufficient Conditions for Power Flow Insolubility Considering Reactive Power Limited Generators with Applications to Voltage Stability Margins", *IIEP*, August 2013, Greece.
- [14] T. J. Overbye, "A power flow measure for unsolvable cases", *IEEE Transactions on Power Systems*, vol. 9, no. 3, pp. 1359-1356, 1994.
- [15] S. Yu, H. D. Nguyen, K. Turitsyn, "Simple certificate of solvability of power equations for distribution systems", *IEEE PES General Meeting*, Denver, CO, USA, 2015.
- [16] H. D. Nguyen, K. Turitsyn, "Appearance of multiple stable load flow solutions under power flow reversal conditions", *IEEE PES General Meeting*, Washington DC, 2014.
- [17] A. Trias, "The holomorphic embedding load flow method", *IEEE PES General Meeting*, 2012, July 2012, pp. 1-8.
- [18] I. Wallace, D. Roberts, A. Grothey, K. I. M. McKinnon "Alternative PV Bus Modeling with Holomorphic Embedding Load Flow Method", *ArXiv e-prints*, July 2016.
- [19] D. Bromberg, M. Jereminov, L. Xin, G. Hug, L. Pileggi, "An Equivalent Circuit Formulation of the Power Flow Problem with Current and Voltage State Variables", *PowerTech Eindhoven, June 2015*.
- [20] W. J. McCalla, "Fundamentals of Computer-Aided Circuit Simulation", Kluwer Academic Publishers, Boston, 1988.
- [21] S.W. Director, R. Rohrer, "The Generalized Adjoint Network and Network Sensitivities", *IEEE Trans. on Circuit Theory*, vol. 16-3, 1969.
- [22] S.W. Director, R. Rohrer, "Automated Network Design-The Frequency Domain Case", *IEEE Trans. on Circuit Theory*, vol. 16, no3, August 1969.
- [23] S. Boyd, L. Vandenberghe, *Convex Optimization*, Cambridge University Press, New York, NY, USA, 2004.
- [24] M. Jereminov, A. Pandey, D. M. Bromberg, X. Li, G. Hug, L. Pileggi, "Steady-State Analysis of Power System Harmonics Using Equivalent Split-Circuit Models", *ISGT Europe*, Ljubljana, October 2016.
- [25] M. Jereminov, D. M. Bromberg, A. Pandey, X. Li, G. Hug, L. Pileggi, "An Equivalent Circuit Formulation for Three-Phase Power Flow Analysis of Distribution Systems", *IEEE T&D Dallas, 2016*.
- [26] Y. Wang, L.C.P. DaSilva, W. Xu, Y. Zhang, "Analysis of ill-conditioned power flow problems using voltage stability methodology", *IEEE Proc. in Generation, T&D*, Vol. 148-5, September 2001.
- [27] R. Zimmerman, C. Murillo-Sanchez, R. Thomas, "MATPOWER: Steady-state operations, planning and analysis tools for power systems research and education", *IEEE Trans. on Power Systems*, vol. 26, no.1, Feb 2011.
- [28] C. Jozs, S. Fliscounakis, J. Maeght, P. Panciatici, "AC Power Flow Data in MATPOWER and QCQP Format: iTesla RTE Snapshots and PEGASE". *ArXiv e-prints*, March 2016.
- [29] A. B. Birchfield, T. Xu, T. Overbye, "Power Flow Convergence and Reactive Power Planning in Creation of Large Synthetic Grids", *IEEE Trans. on Power Systems*, 2018.
- [30] Transmission System Planning Performance Requirements, NREC Standard TPL-001-4, 2015.